Hindawi Publishing Corporation
ISRN Metallurgy
Volume 2013, Article ID 808413, 6 pages
http://dx.doi.org/10.1155/2013/808413

Research Article

High-Temperature (1700–1800°C) Electrochemical Preparation of Metallic Ti from Rutile: A Pathway of Step-by-Step Electrodeoxidization

Fanke Meng and Huimin Lu

School of Materials Science and Engineering, Beihang University, No. 37 Xueyuan Road, Haidian District, Beijing 100191, China

Correspondence should be addressed to Huimin Lu; lhm0862002@gmail.com

Received 7 January 2013; Accepted 3 February 2013

Academic Editors: K. Ameyama, M. Carboneras, T. Czujko, P. Markovsky, and J.-Y. Uan

The mechanism of producing metallic titanium by electrochemically reducing rutile (TiO_2) at high temperatures was studied. First, the oxygen was successfully electroremoved from TiO_2 at temperatures 1700, 1750, and 1800°C in molten CaF_2 under a stable electrolytic potential of 2.5 V. Second, the electrodeoxidization process was studied with cyclic voltammetry (CV) tests at 1750°C. It was found that the electrochemical reduction for preparing metallic Ti from TiO_2 at the high temperatures can be divided into several steps. In other words, the oxygen in TiO_2 was electro-removed as a step-by-step pathway ($TiO_2 \rightarrow Ti_4O_7 \rightarrow Ti_3O_5/Ti_2O_3 \rightarrow TiO \rightarrow Ti$) at different electrolytic potentials. It unraveled the mechanism of electrochemical reduction of TiO_2 at the high temperatures, which is helpful for monitoring the reduction procedure.

1. Introduction

Titanium and its alloys play an essential role in industry because of their excellent properties of high ratio of strength/weight, fine plasticity, and superior corrosion-resistance [1]. Although Ti has an attractive future in industry, it cannot be widely used due to the high cost and complex production procedure. Until now, the mainly used commercial procedure for Ti production is Kroll process [2], but the Kroll process needs large energy and long time. In the recent decade, FFC Cambridge process was proposed and considered to be an effective alternative method of direct electrochemical reduction of rutile (TiO_2) to Ti [3, 4]. In this process, the cathode of TiO_2 pellets was immersed into molten $CaCl_2$ and reduced to Ti electrochemically at 900°C under the electrolytic potentials of 2.8–3.2 V. The electrolytic reactions given by this process can be summarized as the following equations:

$$MO_X + 2Xe^- = M + XO^{2-} \quad \text{at the cathode} \tag{1}$$

$$2O^{2-} - 4e^- + C = CO_2 \quad \text{or}$$
$$O^{2-} - 2e^- + C = CO \quad \text{at the anode} \tag{2}$$

This process has two main advances compared with the traditional Kroll method: first, FFC process is a one-plot technique, thereby less time and less energy are spent; second, it can be applied to produce other metals or alloys by this electrochemical reduction method. For example, until now, many metals and alloys, such as, Cr, Si, Nb, Ni, Zr and Ni-Mn-Ga, Ti-W, and Nb-Si, were produced from their oxides by the electrochemical reduction method [5–14]. However, the most critical challenge to sabotage broad industrial applications of FFC process is low current efficiency and slow reaction rate. For example, the current efficiency was between 30% and 50% in most cases; in only a few experiments it can reach 80% [15]. Moreover, only the TiO_2 contacted with the wrapped electrode wires could be completely deoxidized to metallic Ti after electrochemical reduction for several tens of hours [3]. Perovskite phase ($1.49 < O/Ti < 1.89$) still exists in the areas which are not directly contacted with the electrode wires [16]. The incomplete and time-consuming electrolysis is attributed to relatively lower electrochemical reduction activity at lower experimental temperatures (850–950°C). Moreover, the produced metallic Ti could be covered on the surface of the TiO_2, which would seal the free pathways for oxygen releasing, leading to the termination of the electroreduction process [17, 18].

Recently, elevating electrochemical reduction temperature is considered to be an effective method to increase the efficiency of electrochemical reduction of TiO_2 to produce metallic Ti [19]. Not only was the reaction rate increased by elevating reaction temperature, but also the current efficiency was remarkably rocketed up to 90% [19]. In addition, the electrochemical reduction method at high temperatures (>1500°C) was even used for alloys production, especially for some superalloys [14, 20]. Therefore, the electrochemical reduction method at the high temperatures might be widely used in the future for the production of Ti and other metals or alloys in industry. However, taking the Ti production by high-temperature electrolysis as an example, the mechanism is still unclear. It should be pointed out that the mechanism of electrochemical reduction at high temperature is critical for producing metals or for extracting alloys directly from their oxides.

In this paper, it is the first time to study the mechanism of the electrochemical reduction of TiO_2 to Ti at high temperatures (1700–1800°C). By the cyclic voltammetry (CV) measurement and thermodynamic analysis, we have proven that the electrochemical reduction of TiO_2 has a step-by-step pathway. At an applied experimental temperature, the electrochemical reduction process was dependant on the applied reduction potential.

2. Experimental

2.1. Materials Preparation. In our experiments, CaF_2 is used as electrolyte instead of $CaCl_2$ because the electrolytic temperatures are high [19]. As it is known, the electrolyte can be decomposed if the potential applied is high enough. According to the thermodynamic data in [29], we can calculate that the electrochemical decomposition potential of the $CaCl_2$ is lower than 2.2 V if the electrolysis temperature goes up to 1700°C. The electrochemical decomposition potential of CaF_2, however, is still higher than 4.5 V even in our experimental temperatures (1700–1800°C). In electrolysis, because of unavoidable IR drop, we should select an electrolyte (CaF_2) with a high electrochemical decomposition potential to ensure the fine stability of electrolyte. In this work, CaF_2 (≥99.0%, Chengde Optical & Electrical Materials Ltd., Hebei, China) was prepared as in the following steps: first, CaF_2 powders were die-pressed into small cylindrical pellets under the pressure of 30 MPa; second, the pellets were dried at 70°C in an oven overnight; third, the pellets were pulverized to small grains with an average size less than 5 mm. TiO_2 pellets were prepared from rutile TiO_2 powders (≥99.6%, Chengde Optical & Electrical Materials Ltd., Hebei, China) with an identical method as that used in preparation of the CaF_2 pellets. Then the TiO_2 pellets were pulverized to smaller grains of size less than 1 mm. Graphite crucibles (inner diameter: 9.0 cm, height: 18.0 cm, and wall thickness: 1.0 cm) were flushed with industrial ethanol (>95%, Beijing Keshi Co. Ltd., Beijing, China) for 3–5 times until the inner surfaces were almost free of graphite powders. At last, the TiO_2 grains were placed in the graphite crucible and then covered with CaF_2 grains. Each crucible had about 200 g of TiO_2 and 2000 g of CaF_2.

2.2. Potentiostatic Electrolysis. The CaF_2 was used as electrolyte in both TiO_2 electrolysis and subsequent cyclic voltammetry (CV) measurements. As a cathode, a graphite crucible with TiO_2 and CaF_2 was placed in a temperature-controlled furnace made by China Iron & Steel Research Institute Group, as shown in Scheme 1(a). A graphite anode rod (diameter: 6.0 cm) was hung by an electromotor, which can move up and down vertically to ensure that the graphite rod can contact with the molten electrolyte during the electrolysis. KGHF-1000 A/6 V rectifier, made by Beijing Chunshu Electric rectifier Ltd., Beijing, China, was equipped with the furnace to supply a direct current for the electrolysis. The furnace was vacuumed, and then argon (≥99.9%, O ≤ 10 ppm, H_2O ≤ 15 ppm, and N_2 ≤ 5 ppm) was pumped into the furnace as soon as possible. Purged with the argon for 20 min, all valves of the furnace were turned off. Then the argon flow was kept at a rate of 1.0–1.5 L min^{-1}, and the inlet and outlet valves were adjusted to maintain a gas pressure in the furnace around 0.01 MPa larger than the ambient pressure to further prevent air ingress. Heated the furnace to 500°C with a ramping rate of 20°C min^{-1} and then raised the temperature to 1450°C at an average rate of 10°C min^{-1}. Kept at 1450°C for 30 min to ensure the electrolyte CaF_2 was completely melted in the crucible. Then the temperature continued to rise up to the experimental temperatures of 1700–1800°C with a heating rate of 10°C min^{-1}. Consequently, the potential was set to 2.5 V for electrolysis. It should be pointed out that preelectrolysis in this experiment was not applied as it was in other experiments [3–5, 21, 22]. Residual water and redox in the molten CaF_2 were much less than those in the molten $CaCl_2$, which would be proven by the stable electrolytic current with only mild vibration during electrolysis in the first few minutes. After electrolysis and consequent cooling to room temperature, the graphite crucible was taken out of the furnace. The samples after electrochemical reduction at different high temperatures were obtained by smashing the graphite crucibles.

2.3. CV Measurement. In this work, three-electrode system was used in the CV tests and its design was shown in Scheme 1(b). A Mo wire (diameter: 1.0 mm) and a graphite tablet (4 mm × 10 mm × 50 mm) worked as a quasireference and a counter electrode respectively. The working electrode was TiO_2 slices (2 mm × 10 mm × 40 mm), which were wrapped with a Mo wire (diameter: 0.5 mm). The three electrodes were linked to a CHI 604C Electrochemical System (Shanghai Chenhua Inc., Shanghai, China) with the Mo wires (diameter: 0.5 mm). For fixing the Mo wires, three holes were punched along the axial direction of a graphite rod (diameter: 6.0 cm), which had the same size as the rod used in electrolysis process. Thus, the three electrodes can be hung at the bottom of the graphite rod and move up and down together with the rod. The heating process was the same as that used in the former electrolysis. After reaching the experimental temperature, three electrodes were inserted into molten CaF_2 simultaneously by pushing down the graphite rod for CV measurements.

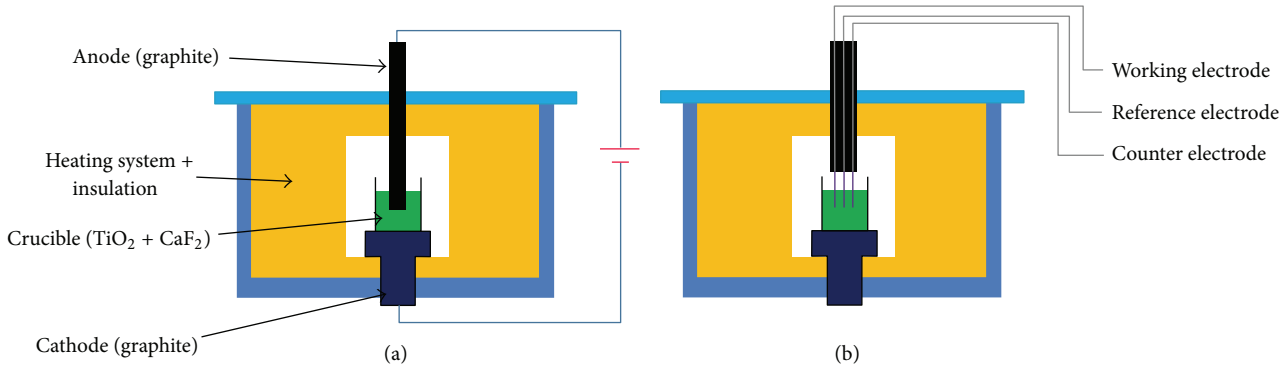

Scheme 1: (a) Schematic of electrolytic cell for TiO_2 electrolysis; (b) design of three-electrode system for cyclic voltammetry (CV) tests.

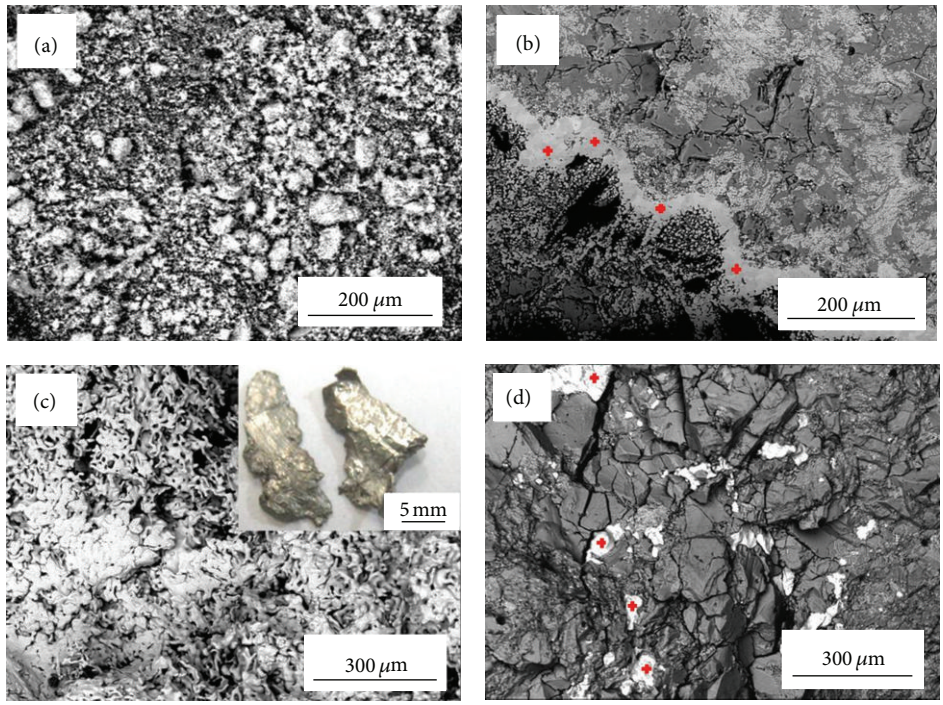

Figure 1: (a) SEM image of TiO_2 powders before electrolysis; SEM images of the samples after electrolysis at (b) 1700°C, (c) 1750°C, and (d) 1800°C, respectively. The inset in (c) shows two selected pieces of metallic Ti slices after electrolysis at 1750°C. Red crosses in (b) and (d) mark the areas for EDX measurement.

2.4. Characterizations of Morphology and Composition. Micrograph and composition analyses were performed with a VEGA\\LMU SEM system equipped with a CCD camera, from TESCAN. EDX equipment was purchased from OXFORD, and the analysis software was INCA.

3. Results and Discussion

Figure 1(a) shows the morphology of pure TiO_2, which were sintered and pulverized into small particles before electrolysis. Most of the particles had a size smaller than 100 μm. Absolutely, the sample before electrolysis was pure TiO_2 by EDX measurement in Table 1. As shown in Figure 1(b), after electrochemical reduction at 1700°C, a bright S-shaped stripe was formed at the bottom of graphite crucible. Left downside areas of the S-shaped stripe, which was close to the bottom of graphite crucible, had large dark areas of graphite. Many scattered small bright areas were located at the right upside of the S-shaped stripe. With EDX measurement of these bright areas in Table 1, the Ti content increased to 75.3 at % but the O content decreased to 9.4 at %, compared with the pure TiO_2. However, the S-shaped stripe still had some Ca and F. Clearly, they were from electrolyte CaF_2. Figure 1(c) shows the sample after electrochemical reduction at 1750°C. Dozens of metallic Ti were obtained by smashing the crucible after electrolysis, among which two selected pieces were shown in the inset of Figure 1(c). Each piece was about 1.5 g in weight. The EDX

Table 1: EDX results of samples before and after electrolysis at different temperatures.

Samples	Ti [at. %]	O [at. %]	Ca [at. %]	F [at. %]
Pure TiO_2[a]	33.2	66.8	—	—
1700°C[b]	75.3	9.4	5.4	9.9
1750°C[c]	100.0	—	—	—
1800°C[b]	91.3	—	3.6	5.1

—Not obtained by EDX.
[a]The sample of pure TiO_2 was measured by EDX before electrolysis.
[b]EDX measurement was taken from the areas in Figures 1(b) and 1(d), respectively. Content of each element was the average value in the four randomly selected areas marked in Figures 1(b) and 1(d), respectively.
[c]EDX result was obtained by surface scanning over the area in Figure 1(c).

results in Table 1 show that the samples obtained after electrolysis at 1750°C were pure metallic Ti. Given that the electrolytic temperatures used in our experiments were just below the melting point of TiO_2 (1843°C) [23], the oxygen ions were easily moved out from TiO_2 crystal lattice. This sample had a porous structure as shown in the SEM image in Figure 1(c). Simultaneously, the porosity structure can supply more free pathways to enhance oxygen ions transport. It should be pointed out that even at lower electrolytic temperatures, the porous structure was also demonstrated [18, 19]. After electrolysis at 1800°C, shown in Figure 1(d), many bright white areas were scattered in grey areas. By checking with the EDX, the large grey areas were electrolyte CaF_2, while the white spots were rich in Ti (91.3 at %) as well as a small amount of Ca and F from electrolyte CaF_2. It demonstrates that the O in TiO_2 was completely removed. However, there are two distinct differences between the sample electrolyzed at 1800°C and that electrolyzed at 1750°C. First, the bright spots, which were rich in Ti, did not aggregate to large pieces of metallic Ti; second, some Ca and F were still contained. This was probably the consequence of intense fluctuation of molten CaF_2 during electrolysis, which resulted from large electrolytic current and high fluidity of electrolyte at high temperatures [24, 25].

Figure 2 shows the chronoamperometric plots of the electrolysis at three different temperatures. Each chronoamperometric plot had a current peak in the first 20–40 min and then decreased to a steady current plateau, which continued for 3-4 hr. The current plateau was almost flat, which indicated that the electrolytic process was stable. Then the electrolytic current dropped to the background current sharply in 5 min. The current behavior can be explained by a three-phase-interline (3PI) mechanism proposed by Deng et al. [26]. Briefly, the electrochemical reduction of insulating solid oxides can proceed at the place of 3PI, linking the conductor, oxide and electrolyte. As reaction persisting, the metal/oxide/electrolyte 3PI propagates, leading to metallization on the 3PI interface initially and then into the interior of oxide preforms until the reduction is completed [5, 6, 27]. Therefore, upon commencing the reduction, total length of the 3PI increased as the current raised. Once the current reached the maximum, the 3PI started to decrease to a steady status, leading to the formation of the current plateaus. Meanwhile, the reaction proceeded into the interior of the oxide until the oxide was completely electroreduced.

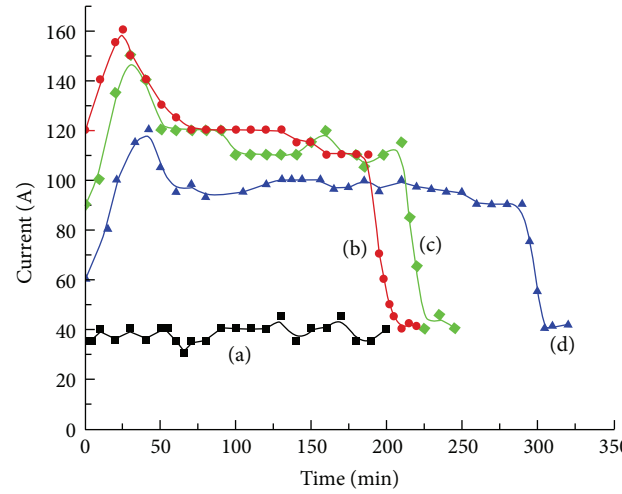

Figure 2: Chronoamperometric plots under constant electrolytic potential of 2.5 V at (b) 1800°C, (c) 1750°C, and (d) 1700°C. Plot (a) is a blank *I-t* curve, obtained under 2.5 V at 1750°C (only electrolyte CaF_2 in the electrolytic graphite crucible).

Thus, the higher the temperature during the electrolysis, the higher the rate of the 3PI propagation, and the earlier the current peak appeared. In addition, the initial electrolytic current peak and current plateau became higher and the total electrolytic time was shortened as the temperature increased.

The design of the three electrodes, shown in Scheme 1(b) and the inset of Figure 3(a), was used for CV tests to demonstrate the electrochemical reduction process of TiO_2. Figure 3 shows the CV curves at 1750°C with and without TiO_2 slices as working electrode in molten CaF_2, respectively. Herein, the equilibrium potential of Ca^{2+}/Ca ($Ca^{2+} + 2e^- \leftrightarrow Ca$; Ca^{2+} and Ca are in standard status) is defined as the reference potential ($E^{\theta}_{Ca^{2+}/Ca} = 0$) as described in the other literature [3, 22, 28]. In Figure 3(a), with the potential becoming positive, oxidation currents increased rapidly to form a peak c1, which was the consequence of Ti dissolution [3]. If the working electrode was changed to a piece of Mo foil without TiO_2 slices, only two current plateaus of c2 and c3 would appear in both positive and negative potential directions, as shown in Figure 3(b). The difference between these two CV curves was a family of current peaks (a1–a5) shown in Figure 3(a). Apparently, these peaks were attributed to many electrochemical reactions. Moreover, we found that many types of titanium oxides existed in the Ti-O binary phase diagram due to different O ratios [23]. According to the O ratios in TiO_2, the reduction process can be divided into many steps, which were shown in (3)–(7):

$$4TiO_2 + 2e^- = Ti_4O_7 + O^{2-}, \quad (3)$$

$$3Ti_4O_7 + 2e^- = 4Ti_3O_5 + O^{2-}, \quad (4)$$

$$2Ti_3O_5 + 2e^- = 3Ti_2O_3 + O^{2-}, \quad (5)$$

$$Ti_2O_3 + 2e^- = 2TiO + O^{2-}, \quad (6)$$

$$TiO + 2e^- = Ti + O^{2-}. \quad (7)$$

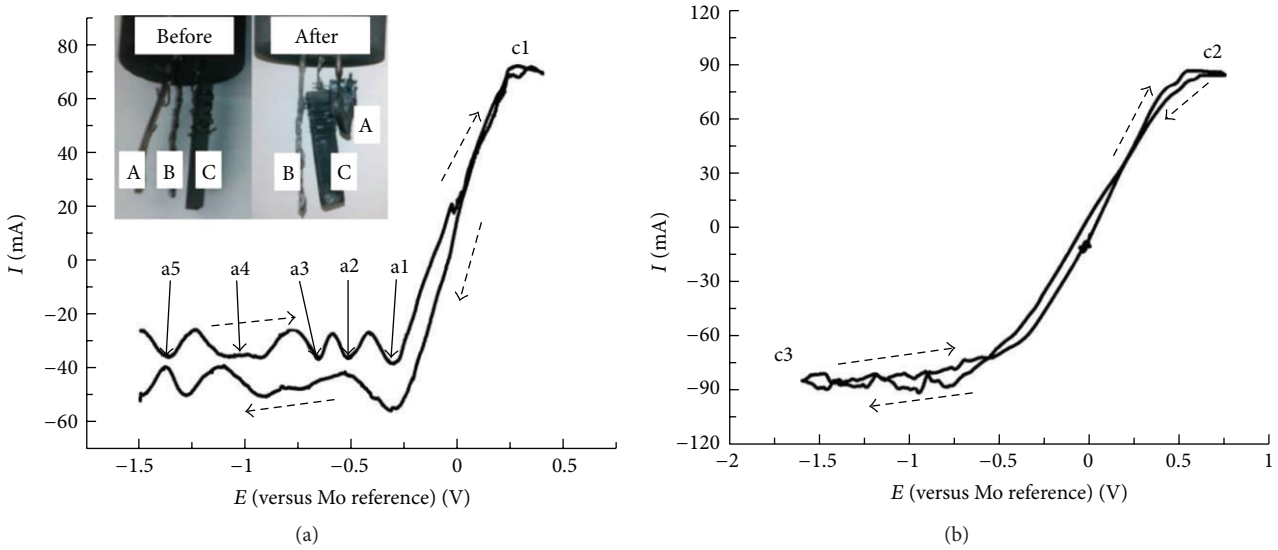

FIGURE 3: CV curves obtained at 1750°C. (a) A TiO_2 slice (from oxidizing Ti foil at 1300°C for 1.5 hr) wrapped with Mo wire as working electrode (the inset of (a) shows the design of three electrodes (working electrode (A), reference electrode (B), and counter electrode (C)) before and after CV test at 1750°C); (b) only Mo foil as working electrode. The scan rate was 20 mV s^{-1}.

According to the thermodynamic data [29], we can obtain the plots of the electrolytic potential against temperature (*E*-*T*), as shown in Figure 4. The theoretical reduction potentials of TiO_2, Ti_4O_7, T_3O_5, Ti_2O_3, and TiO at 1750°C were located at −1.30 V, −1.08 V, −0.96 V, −0.69 V, and −0.23 V, respectively. As what we have discussed above, the current peaks of the CV curve in Figure 3(a) have indicated a series of reactions during the electrochemical reduction process of TiO_2. Obviously, the peaks a5 (−1.28 V), a3 (−0.65 V), and a1 (−0.27 V) in Figure 3(a) were consistent with the theoretical potentials of electrochemical reduction of TiO_2, Ti_2O_3, and TiO, respectively. Therefore, it can be concluded that these three peaks resulted from reactions (3), (6), and (7). Besides, a broad peak (a4) ranged from −0.9 V to −1.13 V, indicating many reactions in this potential range. From the Ti-O binary phase diagram [23], there are a series of phases named Magnéli phases (Ti_nO_{2n-1} ($n \geq 4$)) with an O ratio between Ti_2O_3 and TiO_2. Definitely, the Ti_4O_7 is one of the Magnéli phases. As shown in Figure 4, the titanium oxide with a higher oxygen ratio will have a higher electrochemical reduction potential and vice versa. Therefore, the electrochemical reduction potentials of the Magnéli phases are among Ti_2O_3 and TiO_2. Besides, the reduction potential of the Ti_3O_5 should also be located between Ti_2O_3 and TiO_2. Thereby, the broad peak a4 was composed of reduction peaks of a series of Magnéli phases (Ti_4O_7 is the typical oxidation) and Ti_3O_5. Besides, one point should be highlighted here: the electrochemical reduction potentials of reactions (4) and (5) are very close to each other, as shown in Figure 4. This also indicates why the current peaks can be largely overlapped and merged to one broad peak (a4 in Figure 3(a)). People might question why there is another current peak a2 appeared at −0.51 V since no more Ti-O phases exist between TiO and Ti_2O_3 in the Ti-O binary phase diagram [23]. In fact, TiO can easily form $CaTiO_3$ or other higher perovskite phases

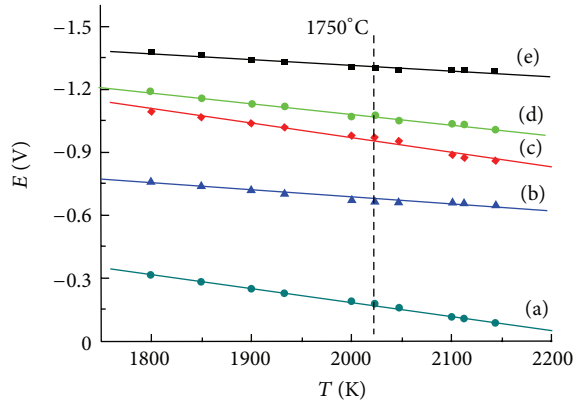

FIGURE 4: Plots of electrochemical reduction potentials of Ti oxides against temperatures: (a) $TiO + 2e^- = Ti + O^{2-}$; (b) $Ti_2O_3 + 2e^- = 2TiO + O^{2-}$; (c) $2Ti_3O_5 + 2e^- = 3Ti_2O_3 + O^{2-}$; (d) $3Ti_4O_7 + 2e^- = 4Ti_3O_5 + O^{2-}$; (e) $4TiO_2 + 2e^- = Ti_4O_7 + O^{2-}$. The vertical dashed line indicates the electrochemical reduction potentials of different Ti oxides at 1750°C.

($Ca_\delta TiO_\chi$ ($\chi/\delta \geq 2$)) with Ca^{2+} and O^{2-} in molten electrolyte as reaction (8) [16, 22]:

$$Ca^{2+} + TiO + 2O^{2-} - 2e^- = CaTiO_3 \quad (8)$$

Based on the thermodynamic data [29], we can infer that reduction potentials of this series of perovskite phases range from −0.36 V to −0.58 V. Therefore, some TiO will react with Ca^{2+} and O^{2-} at high temperatures to form $CaTiO_3$ or other higher perovskite phases, which will lead to the peak a2. The remaining TiO will continue the electrochemical reduction process to be reduced to metallic Ti, leading to the current peak a1 as discussed above.

4. Conclusions

Generally, TiO_2 was successfully electrochemically reduced to metallic Ti at high temperatures (1700–1800°C). The best result was shown by electrolysis at 1750°C; pure metallic Ti pieces were obtained. In addition, we have measured the procedure of the electrolytic reaction at 1750°C. It was found that the electrochemical reduction was separated into several steps. The oxygen in the TiO_2 was electroremoved as a step-by-step pathway ($TiO_2 \rightarrow Ti_4O_7 \rightarrow Ti_3O_5/Ti_2O_3 \rightarrow TiO \rightarrow$ Ti) at different applied reduction potentials. This mechanism of electrochemical reduction can be helpful in controlling the production procedure of Ti in industry. Also, it can be used for producing Ti alloys by electrochemical reduction method at high temperatures.

Acknowledgments

The authors are grateful to the Science and Technology Ministry of China for the financial support to the national high technology project.

References

[1] J. L. Xu and Z. X. Qiu, *Brief Introduction to Direct Reduction of Titanium Dioxide to Titanium Technology*, Metallurgical Industry Press, Beijing, China, 3rd edition, 2004.

[2] W. J. Kroll, "The production of ductile titanium," *Transactions of the American Electrochemical Society*, vol. 78, no. 1, pp. 35–47, 1940.

[3] G. Z. Chen, D. J. Fray, and T. W. Farthing, "Direct electrochemical reduction of titanium dioxide to titanium in molten calcium chloride," *Nature*, vol. 407, no. 6802, pp. 361–364, 2000.

[4] I. Park, T. Abiko, and T. H. Okabe, "Production of titanium powder directly from TiO_2 in $CaCl_2$ through an Electronically Mediated Reaction (EMR)," *Journal of Physics and Chemistry of Solids*, vol. 66, no. 2–4, pp. 410–413, 2005.

[5] G. Z. Chen, E. Gordo, and D. J. Fray, "Direct electrolytic preparation of chromium powder," *Metallurgical and Materials Transactions B*, vol. 35, no. 2, pp. 223–233, 2004.

[6] T. Nohira, K. Yasuda, and Y. Ito, "Pinpoint and bulk electrochemical reduction of insulating silicon dioxide to silicon," *Nature Materials*, vol. 2, no. 6, pp. 397–401, 2003.

[7] K. Yasuda, T. Nohira, and Y. Ito, "Effect of electrolysis potential on reduction of solid silicon dioxide in molten $CaCl_2$," *Journal of Physics and Chemistry of Solids*, vol. 66, no. 2–4, pp. 443–447, 2005.

[8] X. Y. Yan and D. J. Fray, "Production of niobium powder by direct electrochemical reduction of solid Nb_2O_5 in a eutectic $CaCl_2$-NaCl melt," *Metallurgical and Materials Transactions B*, vol. 33, no. 5, pp. 685–693, 2002.

[9] X. Y. Yan and D. J. Fray, "Electrochemical studies on reduction of solid Nb_2O_5 in molten $CaCl_2$–NaCl eutectic," *Journal of The Electrochemical Society*, vol. 152, no. 1, pp. D12–D21, 2005.

[10] G. Qiu, M. Ma, D. Wang, X. Jin, X. Hu, and G. Z. Chen, "Metallic cavity electrodes for investigation of powders electrochemical reduction of NiO and Cr_2O_3 powders in molten $CaCl_2$," *Journal of the Electrochemical Society*, vol. 152, no. 10, pp. E328–E336, 2005.

[11] A. M. Abdelkader, A. Daher, R. A. Abdelkareem, and E. El-Kashif, "Preparation of zirconium metal by the electrochemical reduction of zirconium oxide," *Metallurgical and Materials Transactions B*, vol. 38, no. 1, pp. 35–44, 2007.

[12] A. J. Muirwood, R. C. Copcutt, G. Z. Chen, and D. J. Fray, "Electrochemical fabrication of nickel manganese Gallium alloy powder," *Advanced Engineering Materials*, vol. 5, no. 9, pp. 650–653, 2003.

[13] K. Dring, R. Bhagat, M. Jackson, R. Dashwood, and D. Inman, "Direct electrochemical production of Ti-10W alloys from mixed oxide preform precursors," *Journal of Alloys and Compounds*, vol. 419, no. 1-2, pp. 103–109, 2006.

[14] F. K. Meng and H. M. Lu, "Direct electrochemical preparation of NbSi alloys from mixed oxide preform precursors," *Advanced Engineering Materials*, vol. 11, no. 3, pp. 198–201, 2009.

[15] E. Gordo, G. Z. Chen, and D. J. Fray, "Toward optimisation of electrolytic reduction of solid chromium oxide to chromium powder in molten chloride salts," *Electrochimica Acta*, vol. 49, no. 13, pp. 2195–2208, 2004.

[16] K. Jiang, X. H. Hu, M. Ma et al., "'Perovskitization'-assisted electrochemical reduction of solid TiO_2 in molten $CaCl_2$," *Angewandte Chemie*, vol. 45, no. 3, pp. 428–432, 2006.

[17] W. Li, X. B. Jin, F. L. Huang, and G. Z. Chen, "Metal-to-oxide molar volume ratio: the overlooked barrier to solid-state electroreduction and a "Green" bypass through recyclable NH_4HCO_3," *Angewandte Chemie*, vol. 49, no. 18, pp. 3203–3206, 2010.

[18] F. Scholz, "Nobody can drink from closed bottles, or why it is so difficult to completely reduce solid TiO_2 to solid Ti," *ChemPhysChem*, vol. 11, no. 10, pp. 2078–2079, 2010.

[19] F. Cardarelli, "World intellectual property organization," Patent no. WO 03/046258 A2.

[20] F. K. Meng and H. M. Lu, "tudy on a new electrolysis technology of preparing high Nb bearing TiAl alloy from metal oxides," in *EPD Congress Proceedings*, pp. 711–717, 2009.

[21] G. Z. Chen and D. J. Fray, "Voltammetric studies of the oxygen-titanium binary system in molten calcium chloride," *Journal of the Electrochemical Society*, vol. 149, no. 11, pp. E455–E467, 2002.

[22] K. Dring, R. Dashwood, and D. Inman, "Voltammetry of titanium dioxide in molten calcium chloride at 900∘C," *Journal of the Electrochemical Society*, vol. 152, no. 3, pp. E104–E113, 2005.

[23] J. L. Murray and H. A. Wriedt, *Materials Properties Handbook: Titanium Alloys*, ASM International, Ohio, USA, 1994.

[24] G. Xie, *Theory and Application of Molten Salts*, Metallurgical Industry Press, Beijing, China, 1998.

[25] M. J. Zhang, *Molten Slats Electrochemistry Principle and Application*, Chemical Industry Press, Beijing, China, 2006.

[26] Y. Deng, D. Wang, W. Xiao, X. Jin, X. Hu, and G. Z. Chen, "Electrochemistry at conductor/insulator/electrolyte three-phase interlines: a thin layer model," *Journal of Physical Chemistry B*, vol. 109, no. 29, pp. 14043–14051, 2005.

[27] G. Z. Chen and D. J. Fray, "Understanding the electro-reduction of metal oxides in molten salts," *Light Metals*, pp. 881–886, 2004.

[28] D. T. L. Alexander, C. Schwandt, and D. J. Fray, "The electro-deoxidation of dense titanium dioxide precursors in molten calcium chloride giving a new reaction pathway," *Electrochimica Acta*, vol. 56, no. 9, pp. 3286–3295, 2011.

[29] D. L. Ye, *Handbook of Thermodynamic Data of Practical Inorganic Substances*, Metallurgical Industry Press, Beijing, China, 2nd edition, 2002.